The Amino-Terminal Nine Amino Acid Sequence of Poliovirus Capsid VP4 Protein Is Sufficient To Confer N-Myristoylation and Targeting to Detergent-Insoluble Membranes†

Fernando Martín-Belmonte,‡ José A. López-Guerrero,‡ Luis Carrasco, and Miguel A. Alonso*

Centro de Biología Molecular "Severo Ochoa", Universidad Autónoma de Madrid and Consejo Superior de Investigaciones Científicas, Cantoblanco, 28049 Madrid, Spain

Received September 13, 1999; Revised Manuscript Received November 12, 1999

ABSTRACT: The confinement of membrane proteins by lipid−lipid interactions into specialized detergent-insoluble membrane (DIM) microdomains has been proposed as a general mechanism to recruit selectively lipid-modified proteins and specific transmembrane proteins. Poliovirus capsid VP4 protein and its precursors are myristoylated at the NH_2-terminal Gly residue. To determine whether poliovirus uses DIMs during its replicative cycle, we isolated DIMs from poliovirus-infected HeLa cells and identified the presence of capsid proteins and their precursors, proteinases 2A and 3C, and other viral proteins involved in poliovirus RNA replication such as protein 2C and the polymerase 3D. The morphology of these DIMs was similar to that of the previously described rosettelike vesicles associated with replication complexes isolated from poliovirus-infected cells. To examine the possible role of the myristoyl moiety in the targeting of poliovirus structural proteins to DIMs, we generated a chimeric protein consisting of the nine amino-terminal amino acids from VP4 fused to the amino terminus of the green fluorescent protein (GFP). The selected VP4 sequence was sufficient to confer N-myristoylation and targeting to DIMs to the GFP chimera. Mutations within this sequence known to affect both myristoylation and poliovirus assembly abrogated the targeting of the GFP chimera. These results indicate that the myristoylated amino-terminal nonapeptide from poliovirus VP4 protein constitutes a signal for incorporation into DIMs.

A mechanism based on lipid−lipid or lipid−protein interactions is emerging as one of the strategies used by the cell to recruit specific proteins into specialized membranes (*1*). Proteins attached to the membrane via a lipid anchorage, such as glycosylphosphatidylinositol- (GPI-)[1] anchored proteins and acylated Src-like kinases *(2, 3*) and heterotrimeric Gα subunits (*4*) as well as a restricted number of integral membrane proteins (*5*−*8*), are specifically recruited into specialized membrane microdomains resistant to nonionic detergent (e.g., Nonidet P-40, Triton X-100) solubilization at low temperature. The resistance of these membranes to solubilization seems to be due to their particular lipid composition, which has a high content of both glycolipids and cholesterol (*2, 9*). According to this model, the compatibility of proteins with the detergent-insoluble membrane (DIM) microenvironment provides the biophysical basis for protein recruitment, whereas proteins incompatible with those membranes are excluded.

Formation of viral progeny involves recruitment of structural proteins into specific sites, assembly of these proteins into intermediate capsid scaffolds, and encapsidation of the viral genome. The complexity of the whole process depends on many different factors including virus-specific characteristics such as the number of structural proteins, the existence or not of a viral envelope, and the number of genomic pieces to be encapsidated. The process of concentration of proteins for virus assembly is reminiscent of sorting events occurring in the secretory and endocytic pathways in which specific proteins are segregated from the rest of the cellular proteins and concentrated into definite membrane sites for transport (*10, 11*). Despite the importance of viral model systems as tools to unravel the mechanisms of cell polarity (*10*), little is known about the processes that take place to recruit structural proteins for virus assembly.

Poliovirus, a member of the Picornaviridae family, is a nonenveloped icosahedral virus consisting of 60 copies of each capsid protein (VP1, VP2, VP3, and VP4) and a single-stranded RNA genome of positive polarity. Translation of the genomic RNA generates a 247 000 Da polyprotein that is cotranslationally processed into three precursors (P1, P2, and P3). P1 is the precursor of capsid proteins, whereas P2 and P3 proteolysis originates nonstructural proteins involved in vegetative viral functions (*12*). P1 is released from the polyprotein by the autocatalytic activity of viral proteinase 2A. The viral proteinase 3CD processes the P1 protein to produce the capsid proteins VP0, VP3, and VP1, which form the 5S protomer. To produce mature viral particles, five

† This work was supported by grants from the Dirección General de Enseñanza Superior (PM96-0004) and the Comunidad de Madrid (08.3/0020/1998) to M.A.A. and from the Dirección General de Investigación Científica y Tecnológica (PB94-0148) to L.C. An institutional grant from the Fundación Ramón Areces to the Centro de Biología Molecular "Severo Ochoa" is acknowledged. F.M.-B. is the recipient of a predoctoral fellowship from the Comunidad de Madrid.

* Corresponding author: Tel 34-91-397 8037; Fax 34-91-397 8087; E-mail maalonso@cbm.uam.es.

‡ F.M.-B. and J.A.L.-G. contributed equally to this study.

[1] Abbreviations: DIM, detergent-insoluble membrane; GFP, green fluorescent protein; GPI, glycosylphosphatidylinositol; mAb, monoclonal antibody; PBS, phosphate-buffered saline.

10.1021/bi992132e CCC: $19.00
Published on Web 01/13/2000

protomers give rise to a 14S pentamer and 12 of these pentamers assemble to form a provirion while incorporating the genomic RNA. During maturation of the virion, VP0 is cleaved to form capsid proteins VP4 and VP2 (*12*). The NH_2-terminal glycine from capsid protein VP4 as well as of its precursors, VP0 and P1, is covalently modified by myristic acid (*13, 14*). The myristoylation process occurs cotranslationally (*15*) and is essential for virus growth (*16*−*21*). Consistently, myristoylation-negative poliovirus mutants display defects in assembly (*16*−*20*). The myristic acid moiety participates in important structural interactions within the mature virion particle (*13*). In addition, this lipid moiety appears to be important at multiple stages of poliovirus assembly (*20*) but its exact role in the poliovirus growth cycle remains unknown.

We have examined whether poliovirus uses DIMs during its replicative cycle. Our current results show that poliovirus structural proteins and some other viral proteins accumulate in membranes displaying the biochemical features of DIMs. The morphology of these membranes, as examined by transmission electron microscopy, closely resembles that of the reported poliovirus replication membranous complexes (*22, 23*). Taking into account that the poliovirus capsid proteins are synthesized as a myristoylated precursor, we have investigated the possible role of the lipid moiety in targeting to DIMs. The NH_2-terminal nine amino acid sequence of poliovirus VP4 protein appended to the green fluorescent protein (GFP) (*24*) was able to confer N-myristoylation to the chimera and to target it to DIMs in a myristoylation-dependent fashion. These results, together with the previously reported data showing the requirement of N-myristoylation for assembly (*16*−*20*), are consistent with a role for N-myristoylation in the recruitment of structural proteins into DIMs for poliovirus assembly.

EXPERIMENTAL PROCEDURES

Materials. The mouse hybridoma producing monoclonal antibody (mAb) 9E10 against the human c-Myc epitope EQKLISEED (*25*) was purchased from the American Type Culture Collection. The mouse mAb 1588 against denatured poliovirus type 1 was a generous gift from Dr. M. Ferguson (National Biological Standards Board, Hertfordshire, U.K.). The antibodies to poliovirus protein 2C were obtained as previously described (*26*). Antibodies to E-cadherin were purchased from Transduction Labs (Nottingham, U.K.). Anti-mouse IgG antibodies conjugated to horseradish peroxidase were supplied by Pierce. Octyl glucoside and Triton X-100 were obtained from Sigma.

Cell Culture and Viral Infections. HeLa and COS-7 cells were grown in Dulbecco's modified Eagle's medium supplemented with 10% newborn calf serum (Life Technologies, Inc.), penicillin (50 units/mL), and streptomycin (50 mg/mL) in an atmosphere of 5% CO_2 and 95% air. Infections of confluent cell monolayers with poliovirus type 1 (Mahoney strain) were performed at 10 plaque-forming units/cell for 1 h at 37 °C to allow adsorption and entry of the virus. After that (taken as time 0 of infection), the inoculum was removed and the cell cultures were incubated at 37 °C for the indicated times in normal medium.

DNA Constructions and Transfections. The GFP from the jellyfish *Aequorea victoria* was tagged at its COOH terminus with sequences encoding the c-Myc epitope by the polymerase chain reaction (PCR) (*27*) using oligonucleotides primers corresponding to the 5′ and 3′ ends of the GFP coding sequence and full-length GFP cDNA (*24*) as template. In addition, the 3′-end primer contained sequences encoding the c-Myc epitope located right before the stop translational codon. The POLWT-GFP chimera was constructed by using a 5′-specific oligonucleotide primer containing the sequence encoding the first nine NH_2-terminal amino acids of poliovirus capsid VP4 protein (plus an ATG translational initiation codon) appended to the sequence corresponding to the first six amino-terminal amino acids of GFP, and the same 3′-end oligonucleotide primer described for the GFP construct. The POL1-GFP and POL2-GFP variants were generated as described for POLWT-GFP but by using a 5′-specific oligonucleotide primer with the appropriate modification. The sequence of the inserted product was verified in all of the constructs to eliminate the possibility of amplification errors. For expression in COS-7 cells, the GFP, POLWT-GFP, POL1-GFP, and POL2-GFP DNA amplification products were cloned into the pCR3 eukaryotic expression vector (Invitrogen). Transfections were performed by electroporation using the Electro Cell Manipulator 600 instrument (BTX, San Diego, CA).

Isolation of Total Membranes and Detergent-Insoluble Membranes. DIMs were prepared essentially as described by Brown and Rose (*2*). Cells grown to confluency in 100-mm dishes were rinsed with phosphate-buffered saline (PBS) and lysed for 20 min at 4 °C in 1 mL of 25 mM Tris-HCl, pH 7.5, 150 mM NaCl, 5 mM EDTA, and 1% Triton X-100. The lysate was scraped from the dishes with a cell lifter, the dishes were rinsed with 1 mL of the same buffer at 4 °C, and the lysate was homogenized by passing the sample through a 22-gauge needle. The lysate was finally brought to a concentration of 40% sucrose (w/w) in a final volume of 4 mL and placed at the bottom of an 8 mL 5−30% linear sucrose gradient. Gradients were centrifuged for 18 h at 39 000 rpm at 4 °C in a Beckman SW41 rotor. Fractions of 1 mL were harvested from the bottom of the tube and aliquots were subjected to immunoblot analysis. Density was determined by measuring the refractive index of the fractions. In some experiments, centrifugation to equilibrium was carried out in discontinuous sucrose density gradients consisting of the bottom 4-mL layer containing the cell lysate in 40% sucrose, overlaid with 6 mL of 30% sucrose and a 2-mL layer of 5% sucrose at the top. After centrifugation, the opalescent band containing DIMs, which migrates in the 5−30% sucrose interface, was harvested from the top (fraction I). The 40% sucrose layer containing the cytosolic proteins and the solubilized proteins was harvested as well (fraction S). For isolation of membranes in the absence of detergent we followed essentially the procedure described by Fiedler et al. (*5*). Briefly, cells were washed with ice-cold PBS, scraped with a cell lifter, and centrifuged at low speed. The pellet was resuspended in 2 mL of 10 mM Hepes, pH 7.4, and 2 mM EGTA and homogenized by passing the sample several times through a 22-gauge needle. Microscopic analysis of the homogenate showed that more than 95% of the cells were disrupted by this treatment whereas the nuclei were still intact. Nuclei were removed by low-speed centrifugation, and the postnuclear supernatant was harvested. The postnuclear supernatant was brought to a concentration

of 40% sucrose and sequentially overlaid with 7.5 mL of 30% sucrose and 3 mL of 5% sucrose in 10 mM Hepes, pH 7.4, and 2 mM EGTA. After centrifugation for 20 h at 38 000 rpm in a SW41 rotor at 4 °C, the opalescent band containing cellular membranes (M), which migrates in the 5−30% sucrose interface, was harvested from the top. The 40% sucrose layer containing soluble proteins (S) was harvested as well.

Metabolic Labeling, Immunoblot, and Immunoprecipitation Analyses. For immunoblot analysis, samples were subjected to SDS−PAGE in 15% acrylamide gels under reducing conditions and transferred to Immobilon-P membranes (Millipore, Bedford, MA). After being blocked with 5% nonfat dry milk and 0.05% Tween-20 in PBS, blots were incubated with 9E10 mAb, used as a culture supernatant diluted 1:2. After several washes, blots were incubated for 1 h with goat anti-mouse IgG antibodies coupled to horseradish peroxidase, washed extensively, and developed with an enhanced chemiluminescence Western blotting kit (ECL, Amersham). Quantitative analyses were done with a computing densitometer.

Metabolic labeling with radioactive amino acids was done with cells starved in culture medium lacking methionine and cysteine for 30 min, and then incubated with 100−500 μCi of a (^{35}S)methionine/cysteine mixture (ICN, Costa Mesa, CA) at 37 °C for the indicated times. After this, the medium was removed and replaced with standard culture medium. (^{3}H)-Myristate labeling was done by incubation of transfected COS-7 cells with 200 μCi/mL (^{3}H)myristate at 37 °C for 1 h in normal medium. To detect (^{35}S) or (^{3}H) incorporation into proteins, dried gels were exposed to Fujifilm imaging plates (Fuji Photo Film Co., Japan). For immunoprecipitation studies, extracts were incubated with an irrelevant control mAb bound to protein G−Sepharose and centrifuged. The supernatant was then subjected to immunoprecipitation by incubation with mAb 9E10 bound to protein G−Sepharose. Immunoprecipitates were washed extensively and subjected to SDS−PAGE under reducing conditions.

Electron Microscopic Analysis. DIMs were adsorbed onto collodion/carbon-coated nickel grids for 3 min at room temperature. After washing, samples were blocked with 1% bovine serum albumin in PBS and incubated with the indicated primary antibody. After removing the excess of antibody, grids were incubated with protein A complexed to colloidal gold particles (BioCell Research Laboratories, Cardiff, U.K.). Samples were then washed extensively and fixed with 2% glutaraldehyde. Counterstaining was performed with 2% aqueous uranyl acetate for 6 min. Grids were examined at 80 kV in a JEOL 1200EX electron microscope. Controls to assess the specificity and the lack of cross-labeling included incubations with control primary antibodies and omission of either of the primary antibodies.

RESULTS

Association of Poliovirus Proteins with Detergent-Insoluble Membranes. HeLa cells infected with poliovirus were labeled with (^{35}S)methionine/cysteine at 4 h postinfection for 1 h and chased for 30 min in normal medium. Under these conditions only viral proteins become metabolically labeled due to the profound shut-off of host protein synthesis induced by poliovirus infection. To analyze the possible presence of poliovirus proteins in DIMs, infected cells were

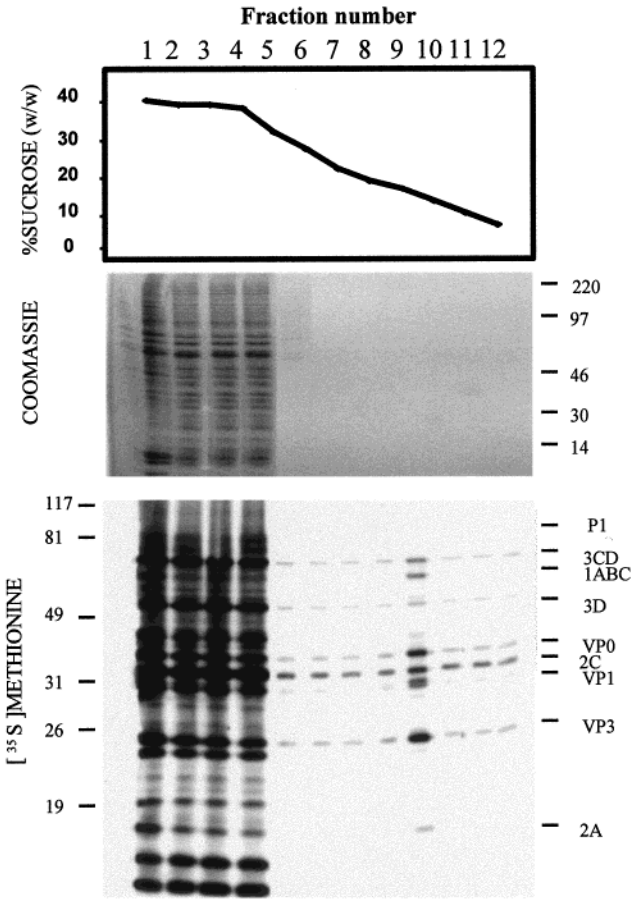

FIGURE 1: Isolation of DIMs from poliovirus-infected cells. HeLa cells were infected with poliovirus for 4 h and metabolically labeled for 1 h at 37 °C with (^{35}S)methionine/cysteine. After washing, cells were chased for 30 min in medium lacking radioactive precursors and extracted with 1% Triton X-100 at 4 °C. The extracts were then centrifuged to equilibrium in sucrose density gradients. Fractions of 1 mL were collected from the bottom of the tube. Density was determined by measuring the refractive index (top panel). Aliquots from each fraction were subjected to SDS−PAGE and stained with Coomassie Blue (middle panel) or analyzed by autoradiography (bottom panel). Fractions 1−4 are the 40% sucrose layer and contain the bulk of cellular membranes and cytosolic proteins, while fractions 5−12 are the 5−30% sucrose layer and contain DIMs. Note that fractions 1−4 include >99% of total cellular proteins. As a control of the fractionation procedure, the analysis of similar fractions from MDCK cells showed that E-cadherin, a membrane protein excluded from DIMs, was present exclusively in fractions 1−4, whereas caveolin, a protein residing in DIMs, peaked in fractions 8−10. The positions of molecular mass markers (middle and bottom panels) and poliovirus proteins (bottom panel) are indicated.

extracted with 1% Triton X-100 at 4 °C, and the extract was centrifuged to equilibrium in sucrose density gradients following an established protocol (*2*). This allows the separation of the low-density buoyant DIM fraction from the bulk of cellular membranes, which are solubilized by the detergent, and from cytosolic proteins. Twelve 1-mL fractions were obtained from the bottom of the tube after fractionation of the gradient. The top panel of Figure 1 shows the density expressed as a percentage of sucrose (w/w) in the different fractions of the gradient. Aliquots from each fraction were subsequently subjected to SDS−PAGE and stained with Coomassie Blue (Figure 1, middle panel). Fractions 1−4, which correspond to the 40% sucrose layer, contain soluble proteins and represent more than 99% of the

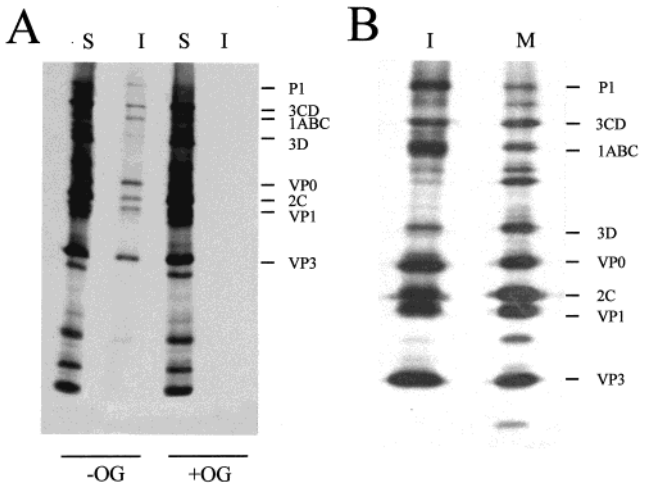

FIGURE 2: Biochemical characterization of membranes isolated from poliovirus-infected cells. HeLa cells infected with poliovirus for 4 h were metabolically labeled for 15 min at 37 °C with (^{35}S)-methionine/cysteine and chased for 5 min in medium lacking radioactive precursors. (A) The Triton X-100-resistant membranes are solubilized by octyl glucoside. Cells were extracted with 1% Triton X-100 either in the absence (−OG) or presence (+OG) of octyl glucoside at 4 °C, and the extracts were centrifuged to equilibrium in a discontinuous sucrose density gradient. The fractions containing the solubilized proteins (S) and the insoluble membranes (I) were harvested, and aliquots were analyzed by SDS−PAGE in a 15% polyacrylamide gel and autoradiographed. (B) The pattern of viral proteins present in DIMs is similar to that in total membrane fractions. Cells were lysed in the absence (M) or presence (I) of 1% Triton X-100 at 4 °C, and the extracts were used to isolate a total membrane fraction (M) or DIMs (I). After separation by SDS−PAGE in a 12% acrylamide gel, equivalent aliquots from the different membrane preparations were autoradiographed. The position of some of the poliovirus proteins is indicated on the right. Note that the apparent difference in the pattern of proteins shown in panels A and B is only due to the percentage of acrylamide used in each case.

total cellular proteins, as shown by quantitative analysis of the stained gel. Fractions 5−12, which represent less than 1% of the total cellular protein, contain DIMs that attain buoyancy under these conditions. Autoradiographic analysis of the labeled proteins (Figure 1, bottom panel) revealed that although the bulk of viral protein was in the soluble fractions, detectable levels of specific viral proteins were also found in the DIM fractions. The most intense bands in these fractions corresponded to the structural proteins VP0, VP1, and VP3 and to the nonstructural protein 2C. In addition, low levels of the virus-encoded proteases 2A and 3CD and of polymerase 3D were also detected in DIMs.

DIMs are known to solubilize in the presence of octyl glucoside (*2*). To assess whether the buoyant membranes containing poliovirus proteins are sensitive to this detergent, infected cells were labeled for 15 min with [^{35}S]methionine/cysteine and chased for 5 min in normal medium. Cells were then extracted either with 1% Triton X-100 alone or with 1% Triton X-100 plus 60 mM octyl glucoside, and the extracts were centrifuged to equilibrium in sucrose density gradients. After gradient fractionation, the soluble and the buoyant fractions were subjected to SDS−PAGE and autoradiographed. Figure 2A shows that in the presence of octyl glucoside no viral proteins were found in the low-density buoyant fractions, supporting the idea of the association of viral proteins with DIMs. The same result was obtained for cells extracted with 1% Triton X-100 at 37 °C (not shown), a second standard treatment used to solubilize DIMs (*2*). Note that, under the labeling conditions used in this experiment, the structural protein precursor P1 was also detected in the DIM fraction (Figure 2A, left panel).

Incorporation of Viral Proteins into DIMs Is Not Caused by the Detergent Extraction Procedure. To compare the pattern of viral proteins present in DIMs with that found in membrane preparations obtained in the absence of detergent, parallel cultures of infected HeLa cells were lysed at 4 °C either in the absence or in the presence of 1% Triton X-100 and were fractionated through a discontinuous sucrose density gradient by centrifugation to equilibrium. The opalescent band at the 5−30% sucrose interface was harvested and equivalent aliquots from the different fractions were analyzed by SDS−PAGE. Figure 2B shows that the viral proteins present in DIMs (I) were also detected in the membranes obtained in the absence of detergent (M). As previously reported (*28*), the structural proteins VP3, VP1, and VP0 and the structural precursors P1 and 1ABC, as well as the nonstructural proteins 2C, 3CD, and 3D, were detected in the total membrane fraction (M).

The DIM Fraction Obtained from Poliovirus-Infected HeLa Cells Consists of Large Membrane Complexes Containing Viral Proteins. To further characterize the DIM fraction, we examined by electron microscopy DIMs isolated from poliovirus-infected HeLa cells. As shown in Figure 3, DIMs from infected cells appeared as a homogeneous population of membranous structures of approximately 100 nm in diameter that were either associated to form larger structures (A) or in an isolated form (C). The morphology of these structures closely resembles that of the isolated rosettelike vesicles containing poliovirus replication complexes (*22, 23*). In agreement with our biochemical results showing the presence of poliovirus structural proteins in the DIM fraction (Figure 1), these rosettelike membranes were shown to contain 14S pentamer capsid precursors (*23*). To address the presence of structural viral proteins in DIMs from poliovirus-infected cells, immunoelectron microscopic analysis was performed by incubating the DIM fraction with an antibody raised against denatured poliovirus particles that recognizes 14S pentamer capsid proteins. Figure 3 panels A and B show that capsid proteins were detected in the DIM structures, whereas no labeling was observed when irrelevant primary antibodies were used (not shown). Furthermore, in agreement with our biochemical results, and with the data obtained for membrane-bound replication complexes (*23*), protein 2C was also found specifically associated with DIMs (Figure 3C).

The NH_2-Terminal Nine Amino Acid Sequence of Poliovirus Protein VP4 Is Sufficient To Confer N-myristoylation to a Reporter Protein. Poliovirus and other members of the Picornaviridae family are modified by myristic acid covalently bound to capsid VP4 protein (*13*). We have adopted the GFP as a reporter protein to address the possible role of N-myristoylation in the targeting of poliovirus structural proteins to DIMs. To this end, we made constructs expressing either GFP or a chimera consisting of the first nine NH_2-terminal amino acids from poliovirus VP4 appended to the amino terminus of GFP (POLWT-GFP). As shown in Figure 4, the selected poliovirus sequence was sufficient to cause myristoylation of the chimeric protein as assayed by in vivo (^{3}H)myristate labeling of COS-7 cells transfected with

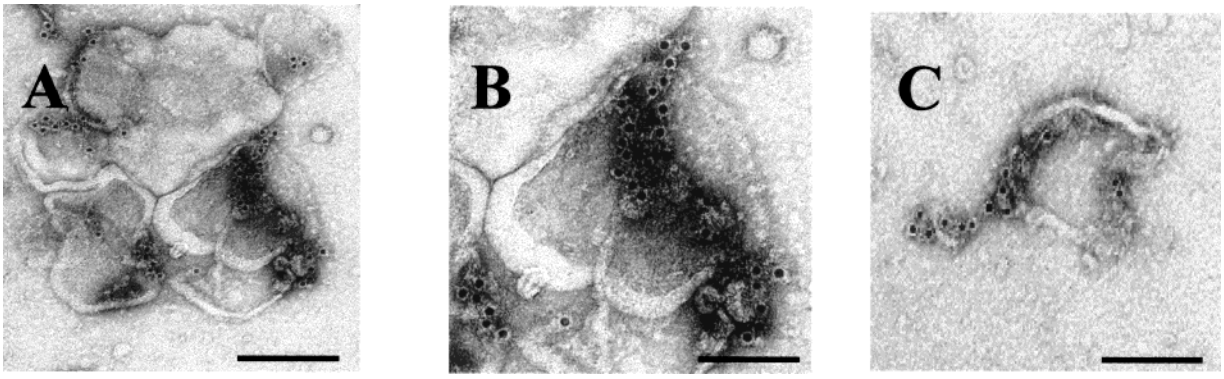

FIGURE 3: Electron microscopic analysis of the DIM fraction isolated from poliovirus-infected cells. HeLa cells infected with poliovirus for 4 h were extracted with 1% Triton X-100 at 4 °C. After centrifugation to equilibrium, the DIM fraction was processed for immunoelectron microscopy with antibodies that recognize 14S pentamer capsid proteins (A, B) or protein 2C (C). After extensive washing, the bound antibodies were visualized with protein A−gold. No labeling was observed in the absence of primary antibody (not shown). Panel B is an enlargement of a selected part of panel A. Bars, 100 nm (A) or 50 nm (B, C).

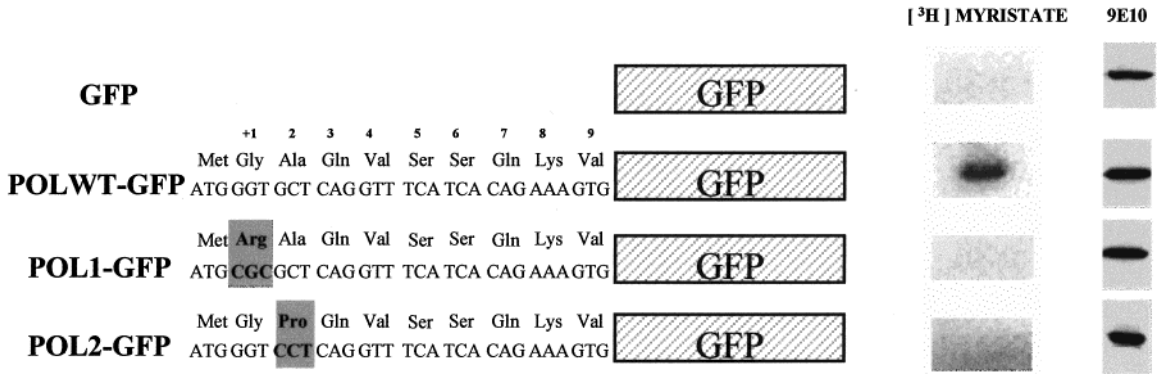

FIGURE 4: The NH_2-terminal nine amino acid sequence of poliovirus capsid protein VP4 fused to the amino terminus of GFP is sufficient to confer myristoylation to the chimeric protein. c-Myc-tagged GFP or chimeric proteins carrying either the wild-type nine NH_2-terminal amino acids of poliovirus capsid protein VP4 (POLWT-GFP) or the indicated variants of these sequence (POL1-GFP and POL2-GFP) were transiently transfected in COS-7 cells. After 24 h, cells were metabolically labeled with (^{3}H)myristic acid for 1 h. After cell lysis, the extracts were immunoprecipitated with anti-tag 9E10 antibodies, and the immunoprecipitates were analyzed by autoradiography after SDS−PAGE, to detect myristoylation, and by immunoblotting with anti-tag 9E10 mAb, to check that the efficiency of the immunoprecipitation was similar in all the samples. No immunoprecipitation of the GFP proteins was detected with a negative control anti-CD3 mAb (not shown). The amino acids from mature VP4 are numbered starting from the NH_2-terminal residue.

POLWT-GFP. As a control, two mutants of POLWT-GFP were constructed to express chimeric proteins carrying Gly^1 to Arg (POL1-GFP) or Ala^2 to Pro (POL2-GFP) mutations in the poliovirus sequence. These mutations are known to abolish poliovirus protein myristoylation (*16*) and, accordingly, prevented myristoylation of the corresponding chimeric proteins (Figure 4).

Myristoylation of Poliovirus VP4 NH_2-Terminal Sequence Is Necessary for Targeting of a Reporter Chimera to Detergent-Insoluble Membranes. Finally, we addressed the question of whether the acylated NH_2-terminal peptide could be a major determinant for the targeting of poliovirus structural proteins and their precursors to DIMs. COS-7 cells transiently expressing each of the constructs were extracted with 1% Triton X-100 at 4 °C, and the extracts were centrifuged to equilibrium in a discontinuous sucrose density gradient. Equivalent aliquots from the initial lysate (T) and from the soluble (S) and the DIM fractions (I) were analyzed by immunoblotting to detect the different GFP chimeras. Figure 5A shows that whereas unmyristoylated GFP, POL1-GFP, and POL2-GFP remained exclusively in the soluble fractions, the myristoylated POLWT-GFP chimera was partially incorporated into DIMs. To rule out the possibility that the inclusion of POLWT-GFP into membranes was caused by the detergent extraction procedure, we isolated membranes (M) and soluble proteins (S) from lysates prepared in the absence of detergent. Figure 5B shows that whereas POLWT-GFP was partially recovered from the membrane fraction, POL1-GFP was confined to the soluble fraction. With GFP and POL2-GFP the same result was obtained as with POL1-GFP (not shown). Finally, as a control of the different fractionation procedures used, the distribution of E-cadherin, an endogenous integral membrane protein that is excluded from DIMs (*8*), was analyzed. As expected, E-cadherin was exclusively found in the membrane fraction obtained in the absence of detergent (Figure 5B) and in the soluble fraction in the samples extracted with 1% Triton X-100 (Figure 5A).

DISCUSSION

A Specific Subset of Poliovirus Proteins Are Present in DIMs Prepared from Infected Cells. The selective inclusion of proteins into DIMs is emerging as a general cellular mechanism for the recruitment of specific proteins into specialized membranes (*1*). In this study, taking advantage of the profound shut-off of host protein synthesis induced during infection, we have examined whether poliovirus, a nonenveloped icosahedral virus of the Picornaviridae family, uses DIMs to segregate specific viral proteins. The analysis of the DIM fraction obtained from poliovirus-infected HeLa

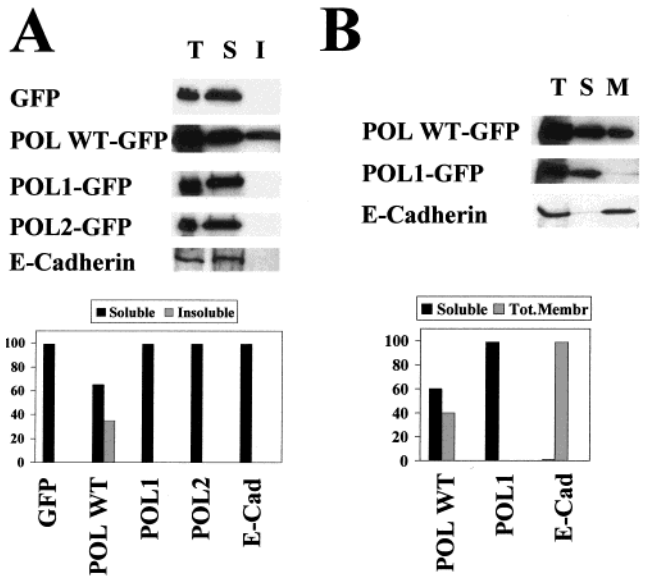

FIGURE 5: The myristoylated NH_2-terminal nine amino acid sequence of poliovirus capsid protein VP4 is sufficient to target a reporter GFP chimera to DIMs. COS-7 cells were transfected with the indicated GFP constructs and harvested 24 h after transfection. (A) The myristoylated NH_2-terminal nine amino acid sequence of poliovirus capsid protein VP4, but not unmyristoylated variants, targets GFP to DIMs. Cells were lysed in the presence of 1% Triton X-100 at 4 °C, and the extracts were centrifuged to equilibrium in a discontinuous sucrose density gradient. The initial lysate (T) and the soluble and the DIM (I) fractions were analyzed by immunoblotting with anti-tag 9E10 antibodies. The histogram represents the percentage of the indicated proteins in the soluble fraction (black bars) and the DIM (insoluble) fraction (shaded bars). The values obtained in three independent experiments did not vary in more than 10% from those shown. (**B**) The presence of myristoylated GFP in membranes is not an artifact of the detergent extraction procedure. Cells expressing either POLWT-GFP or POL1-GFP were lysed in the absence of detergent and used for the preparation of a total membrane fraction. Aliquots from the initial lysate (T) or from the soluble (S) or membrane (M) fractions were subjected to immunoblot analysis with anti-tag 9E10 antibodies. The histogram represents the percentage of the indicated proteins in the soluble fraction (black bars) and the total membrane fraction (shaded bars). The values obtained in three independent experiments did not vary more than 10% from those shown. Immunoblotting with anti-E-cadherin antibodies, an endogenous integral membrane protein excluded from DIMs, was used in panels A and B as an internal control of the fractionation procedures.

cells revealed the presence of capsid proteins and their precursors, as well as that of some nonstructural proteins, in these specialized membranes. However, it is still possible that weak interactions with microdomain lipids cannot be detected after DIM isolation (*29*). The pattern of viral proteins detected in DIMs was similar, with some minor exceptions, to that obtained in membranes prepared in the absence of detergent fraction, indicating that the association of poliovirus proteins with membranes occurs mostly in DIM microdomains. In addition to the structural proteins and precursors, some nonstructural proteins including proteins 2C, 3D, 2A, and 3CD were also detected in DIMs. The presence of low levels of proteases 2A and 3CD is consistent with their respective roles in the cleavage of P1 from the polyprotein precursor and the subsequent hydrolysis of P1 into VP0, VP3, and VP1 (*12*). Both 2C and the poliovirus RNA polymerase 3D are essential for viral replication (*12*), and its presence in DIMs suggests that these membranes might be related to the membranous structures containing RNA replication complexes. Furthermore, 2C has been involved in virus assembly (*30*), and the ATPase activity of 2C has been related to its participation in viral RNA encapsidation (*31, 32*).

DIMs from Poliovirus-Infected Cells Morphologically Resemble Previously Reported Membranous Structures Containing Poliovirus Replication Complexes. Poliovirus infection induces dramatic morphological and biochemical alterations in the host cell. Soon after infection, membranous structures begin to accumulate in the cytoplasm of poliovirus-infected cells (*33*). These structures were described more than three decades ago by Dales et al. (*34*) as small membrane-enclosed bodies of 50−400 nm diameter. Poliovirus RNA replication is coupled to lipid biosynthesis (*35*). Proteins 2C and 2BC appear to play a major role in the proliferation of the membranous vesicular structures that contain viral RNA replication complexes (*36, 37*). Upon isolation, the virus-induced membranous structures coalesce to form rosettes containing replication complexes (*22, 23*). Similarly, it appears that the morphology of the DIM fraction does not represent the actual organization of the membrane microdomains because some microdomains' markers were shown to coalesce upon extraction with Triton X-100 (*38*). Electron microscopic analysis of DIMs from poliovirus-infected cells revealed that their morphology closely resembles that of the isolated rosettelike vesicles associated with replication complexes (*23*). Moreover, our biochemical and immunolocalization data showing the presence of poliovirus capsid proteins and protein 2C as major components of the DIM fraction are consistent with the reported presence of poliovirus structural proteins and protein 2C in the rosettelike vesicles obtained from poliovirus-infected cells (*23*).

The NH_2-Terminal Nine Amino acid Sequence from Poliovirus VP4 Appended to a Reporter Protein Is Sufficient to Confer N-myristoylation and Targeting to DIMs. Although the biological function of the amino-terminal myristyl group in many proteins remains unclear, this covalently attached lipid appears to be important for the intracellular distribution of certain myristoylated proteins (*39*). The expressed chimeras in which GFP was fused at its NH_2-terminus to the first nine NH_2-terminal amino acids of protein VP4, or to variants of this sequence that are known to impede myristoylation of poliovirus VP4, indicate that the poliovirus VP4 NH_2-terminal nine amino acid sequence is sufficient to specify N-myristoylation.

The capacity of the NH_2-terminal sequence of VP4 to interact with DIMs was demonstrated with the GFP chimeras. Our results show that this sequence was sufficient for membrane attachment of the chimera and for incorporation into DIMs. Moreover, myristoylation was required for these effects, as mutations that impair myristoylation render the chimeras unable to attach to membranes. The fact that only a fraction of both VP0 and POLWT-GFP were incorporated into DIMs is consistent with the myristate chain having a lower affinity for membranes than do other lipid moieties (*39, 40*), and it is in agreement with the results obtained in the case of other myristoylated proteins (*41*−*44*). It is possible that the weak interaction of myristate with membranes might facilitate VP4, which is reorganized to be internally located once assembly of new virions has taken place, to lose its contact with DIMs and, thus, lead to virion detachment from membranes.

The Myristate Moiety as a Signal for Recruitment of Capsid Proteins in Specialized Membranes: The Reopening of a Hypothesis for Poliovirus Assembly? The role of poliovirus VP4 myristoylation was previously investigated with a panel of poliovirus mutants with NH_2-terminal modifications either affecting myristoylation of protein VP4 or not (*16*). All of the unmyristoylated mutants analyzed gave rise to inviable phenotypes. Delayed production of virus was occasionally observed that corresponded to revertants that restore NH_2-terminal myristoylation of VP4 as well as a wild-type virus phenotype. Myristoylation negative mutants with the NH_2-terminal Gly residue substituted by either Arg or Ala replicated normally but were deficient in the assembly of 14S pentamers (*19*). Supporting this, there is a strong kinetic preference for myristoylated versus unmodified protomers to assemble into pentamers, and myristoylated pentamers are essential for mature virion formation (*20, 45*). These results suggested that the myristoyl moiety might catalyze the nucleation of pentamers. Although an appealing idea, a role for the myristate modification as a signal for membrane targeting of poliovirus capsid proteins was ruled out by the claim that poliovirus capsid proteins do not associate with membranes (*28*). That claim was based on the observation that the poliovirus structural proteins were not extracted from a total membrane fraction with cold Triton X-100. Taking into account that Triton X-100 insolubility at low temperature is exactly the operational test used to define membranes as DIMs (*2*), a reinterpretation of those results in the light of the current models of protein recruitment is fully consistent with our results showing the presence of poliovirus structural proteins in DIMs.

Our results showing poliovirus capsid protein in the DIM fraction of infected cells, together with the N-myristoylation-dependent incorporation into DIMs of GFP chimeras containing the first nine NH_2-terminal amino acids of VP0, support the hypothesis that VP0 carries a signal for targeting to DIMs. VP1 and VP3 are present in DIMs probably because the folding of P1 allows VP1 and VP3 sequences to interact with the myristoylated VP0 portion before cleavage by protease 3CD. After cleavage, VP0 would remain attached to DIMs through its myristate moiety whereas VP1 and VP3 maintain their association with VP0 forming 5S protomers. The specific recruitment of structural proteins into DIMs would induce a high concentration of protomers and might facilitate the assembly of capsid intermediates. This is consistent with the observation that elimination of the myristoylation signal sequence prevents the assembly of 14S pentamers (*45*). Furthermore, our results showing (1) the presence in DIMs of machinery for poliovirus RNA replication (2C, 3D) and (2) the close morphological resemblance of DIMs obtained from infected cells with the reported rosettelike vesicles containing poliovirus replication complexes suggest that the DIM fraction analyzed by us and the previously described poliovirus replication complexes (*22, 23*) contain identical structures. Pioneer experiments (*46, 47*) implied that poliovirion assembly takes place in the vicinity of the site of RNA replication. Supporting this, coupling between replication and packaging of poliovirus RNA has been recently demonstrated (*48*). Anchorage through myristate to specialized DIMs might (i) allow for membrane-associated P1 processing, (ii) concentrate protomers for building intermediate capsid scaffolds, and (iii) facilitate RNA encapsidation because of the spatial proximity to the site of RNA synthesis (Figure 6). Finally, in the late stages of virion maturation, the myristate moieties would detach from DIMs in a process that might be coupled to VP0 proteolysis to give VP2 and VP4, and the hydrocarbon chain of the myristate moieties may be used to stabilize the mature virion through hydrophobic interactions between them and with capsid VP3 and VP4 proteins (*13*).

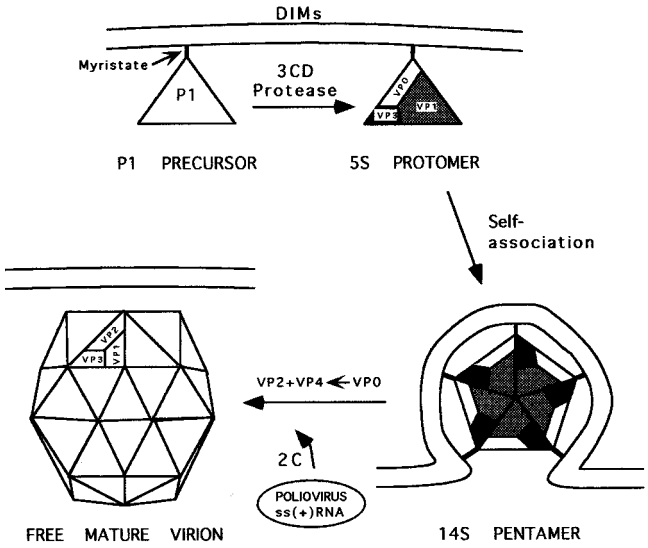

FIGURE 6: Schematic for the proposed role of poliovirus protein myristoylation.

ACKNOWLEDGMENT

We thank María Teresa Rejas for her help in the preparation and analysis of samples for electron microscopy.

REFERENCES

1. Simons, K., and Ikonen, E. (1997) *Nature 387*, 569−572.
2. Brown, D. A., and Rose, J. K. (1992) *Cell 68*, 533−544.
3. Cinek, T., and Horejsi, V. (1992) *J. Immunol. 146*, 4092−4098.
4. Salomon, K., Rudd, C. E., and Finberg, R. W. (1996) *Proc. Natl. Acad. Sci. U.S.A. 93*, 6053−6058.
5. Fiedler, K., Kobsayashi, T., Kurzchalia, T. V., and Simons, K. (1993) *Biochemistry 32*, 6365−6373.
6. Melkonian, K. A., Chu, T., Tortorella, L. B., and Brown, D. A. (1995) *Biochemistry 34*, 16161−16170.
7. Lisanti, M. P., Scherer, P. E., Vidugiriene, J., Tang, Z.-L., Hermanowski-Vosatka, A., Tu, Y.-H., Cook, R. F., and Sargiacomo, M. (1994) *J. Cell Biol. 126*, 111−126.
8. Martín-Belmonte, F., Kremer, L., Albar, J. P., Marazuela, M., and Alonso, M. A. (1998) *Endocrinology 139*, 2077−2084.
9. Hanada, I., Nishijima, M., Akamatsu, Y., and Pagano, R. E. (1995) *J. Biol. Chem. 270*, 6254−6260.
10. Rodriguez-Boulan, E., and Powell, S. K. (1992) *Annu. Rev. Cell Biol. 8*, 395−427.
11. Matter, K., and Mellman, I. (1994) *Curr. Opin. Cell Biol. 6*, 545−554.
12. Ansardi, D. C., Porter, D. C., Anderson, M. J., and Morrow, C. D. (1996) *Adv. Virus Res. 46*, 1−68.
13. Chow, M., Newman, J. F. E., Filman, D., Hogle, J. M., Rowlands, D. J., and Brown, F. (1987) *Nature 327*, 482−486.
14. Paul, A. V., Schultz, A., Pincus, S. E., Oroszlan, S., and Wimmer, E. (1987) *Proc. Natl. Acad. Sci. USA 84*, 2708−2712.
15. Urzainqui, A., and Carrasco, L. (1989) *Biochem. Biophys. Res. Commun. 158*, 263−271.

16. Marc, D., Drugeon, G., Haenni, A. L., Girard, M., and van der Werf, S. (1989) *EMBO J. 8*, 2661−2668.
17. Marc, D., Masson, G., Girard, M., and van der Werf, S. (1990) *J. Virol. 64*, 4099−4107.
18. Krausslich, H.-G., Holscher, C., Reuer, Q., Harber, J., and Wimmer, E. (1990) *J. Virol. 64*, 2433−2436.
19. Marc, D., Girard, M., and van der Werf, S. (1991) *J. Gen. Virol. 72*, 1151−1157.
20. Moscufo, N., Simons, J., and Chow, M. (1991) *J. Virol. 65*, 2372−2380.
21. Ansardi, D. C., Porter, D. C., and Morrow, C. D. (1992) *J. Virol. 66*, 4556−4563.
22. Pfister, T., Pasamontes, L., Troxler, M., Egger, D., and Bienz, K. (1992) *Virology 188*, 676−684.
23. Egger, D., Pasamontes, L., Bolten, R., Boyko, V., and Bienz, K. (1996) *J. Virol. 70*, 8675−8683.
24. Chalfie, M., Tu, Y., Euskirchen, G., Ward, W. W., and Prasher, D. C. (1994) *Science 263*, 802−805.
25. Evan, G. I., Lewis, G. K., Ramsay, G., and Bishop, J. M. (1985) *Mol. Cell. Biol. 5*, 3610−3616.
26. Aldabe, R., Barco, A., and Carrasco, L. (1996) *J. Biol. Chem. 271*, 23134−23137.
27. Sambrook, J., Fritsch, E. F., and Maniatis, T. (1989) *Molecular Cloning: a Laboratory Manual*, second edition, Cold Spring Harbor Laboratory Press, Cold Spring Harbor, NY.
28. Lee, Y. M. H., and Chow, M. (1992) *Virology 187*, 814−820.
29. Harder, T., Scheiffele, P., Verkade, P., and Simons, K. (1998) *J. Cell Biol. 141*, 929−942.
30. Li, J. P., and Baltimore, D. (1990) *J. Virol. 64*, 1102−1107.
31. Rodriguez, P. L., and Carrasco, L. (1993) *J. Biol. Chem. 268*, 8105−8110.
32. Vance, L. M., Moscufo, N., Chow, M., and Heinz, B. A. (1997) *J. Virol. 71*, 8759−8765.
33. Bienz, K., Egger, D., Rasser, Y., and Bossart, W. (1980) *Virology 100*, 390−399.
34. Dales, S., Eggers, H. J., Tamm, I., and Palade, G. E. (1965) *Virology 26*, 379−389.
35. Guinea, R., and Carrasco, L. (1990) *EMBO J. 9*, 2011−2016.
36. Cho, M. W., Teterina, N., Egger, D., Bienz, K., and Ehrenfeld, E. (1994) *Virology 202*, 129−145.
37. Barco, A., and Carrasco, L. (1995) *EMBO J. 14*, 3349−3364.
38. Mayor, S., and Maxfield, F. R. (1995) *Mol. Biol. Cell 6*, 929−944.
39. Bhatnagar, R. S., and Gordon, J. I. (1997) *Trends Cell Biol. 7*, 14−20.
40. McLaughlin, S., and Aderem, A. (1995) *Trends Biochem. Sci. 20*, 272−276.
41. Song, K. S., Sargiacomo, M., Galbiatti, F., Parenti, M., and Lisanti, M. P. (1997*) Cell. Mol. Biol. 43*, 293−303.
42. Zlatkine, P., Mehul, B., and Magee, A. I. (1997) *J. Cell Sci. 110*, 673−679.
43. Liu, J., Hughes, T. E., and Sessa, W. C. (1997) *J. Cell Biol. 137*, 1525−1535.
44. Galbiati, F., Volonté, D., Meani, D., Milligan, G., Lublin, D. M., Lisanti, M. P., and Parenti, M. (1999) *J. Biol. Chem. 274*, 5843−5850.
45. Simons, J., Rogove, A., Moscufo, N., Reynolds, C., and Chow, M. (1993) *J. Virol. 67*, 1734−1738.
46. Girard, M., and Baltimore, D. (1967) *J. Mol. Biol. 24*, 59−74.
47. Caliguri, L. A., and Compans, R. W. (1973) *J. Gen. Virol. 21*, 99−108.
48. Nugent, C. I., Johnson, K. L., Sarnow, P., and Kirkegaard, K. (1999) *J. Virol. 73*, 427−435.

BI992132E